Imaging through turbid media

Hema Ramachandran

Raman Research Institute, C. V. Raman Avenue, Sadashivanagar, Bangalore 560 080, India

In recent years, there has been rapid advance in the field of imaging through turbid media. The technological advances have made possible feats that some years ago would have been thought to be impossible – like looking through flesh with visible light. Some of the techniques developed, and applications of these will be reviewed.

IMAGING through turbid media has, in recent years, become a field of immense research, for its great potential for diverse applications like observing objects through fog, sighting aircraft through clouds, or searching for objects in murky waters. Aviation, defence, astrophysics, marine science and many industries are some of the areas which would benefit from advances in imaging through turbid media. Currently emphasis has mostly been laid on medical applications using infrared or visible light instead of harmful X-rays for imaging through tissues and flesh. Clinical studies have shown that the absorption characteristics at some wavelength by normal tissues differ significantly from some tumours[1] and this behaviour has been adapted for discriminating or locating tumours in the human body. This article will briefly discuss propagation of light in turbid media, and will concentrate on the various techniques devised to image through such media.

Light propagation in turbid media

Fog, milk and other random inhomogeneous media render imaging difficult due to the random multiple scattering of light. Inhomogeneities in the media cause scattering which may alter the direction of propagation, polarization and phase of light. While the propagation of light through such media may be analysed either by means of the wave picture or the photon picture, the latter is more appealing. Photons travel in straight line paths until they encounter an inhomogeneity, when they are scattered in random directions. The scattering is said to be in the Rayleigh regime when the radius, a, of the scatterer, is less than λ, the wavelength of light. In this case, the intensity of scattered light is equal in both the forward and backward directions (Figure 1 *a*). As the size of the particle increases, the scattering is more peaked in the forward direction (Figure 1 *b*). The case of $a > \lambda$, known as the Mie regime, shows peaking in some angles (Figure 1 *c*).

In a turbid medium made up of a random aggregate of scatterers, the photons undergo repeated scattering. The turbid medium is characterized by the scattering mean free path, l_s, which is the mean distance the photons travel before getting scattered, and the transport mean free path, l^*, which is the mean distance photons travel before the direction of propagation is randomized. Since it is quite possible that photons are forward scattered (and continue to travel in the same direction), $l^* > l_s$. The transport mean free path depends upon the number density of scatterers, refractive index contrast between the medium and the scatterers, and the anisotropy factor, i.e. a factor quantifying the directional distribution of scattering. Typical values[2] of l^* for infrared light in tissues are 1–2 mm.

The light emerging from a turbid medium consists of three components – the ballistic, the diffusive and the snake photons. These differ in their paths through the medium, and consequently in their imaging properties. The unscattered or forward scattered photons travel undeviated and emerge the first, having travelled the shortest distance through the medium (Figure 2). These preserve the characteristics of the incident light, namely direction of propagation, polarization and are

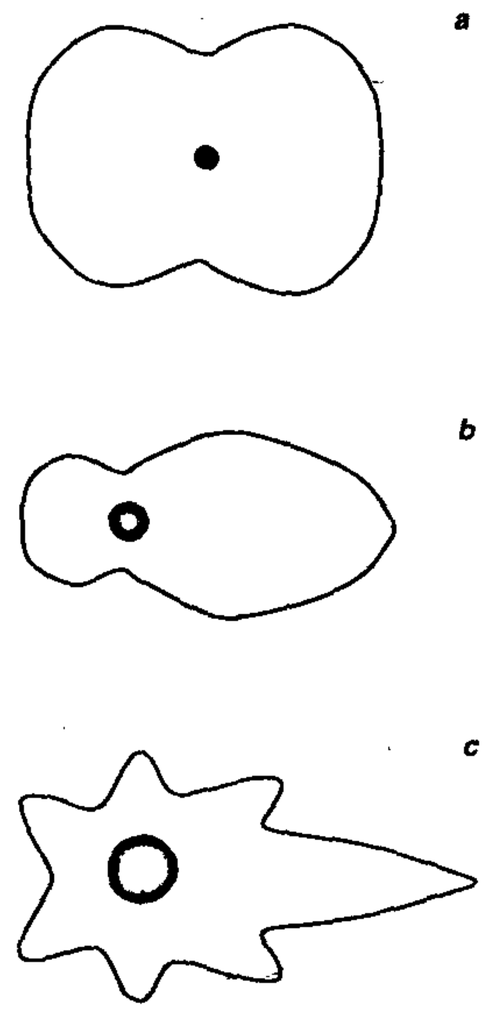

Figure 1. Intensity distribution of scattered light of wavelength λ from a spherical particle of radius a. *a*, $a \ll \lambda$; *b*, $a = \lambda/4$; and *c*, $a \gg \lambda$.

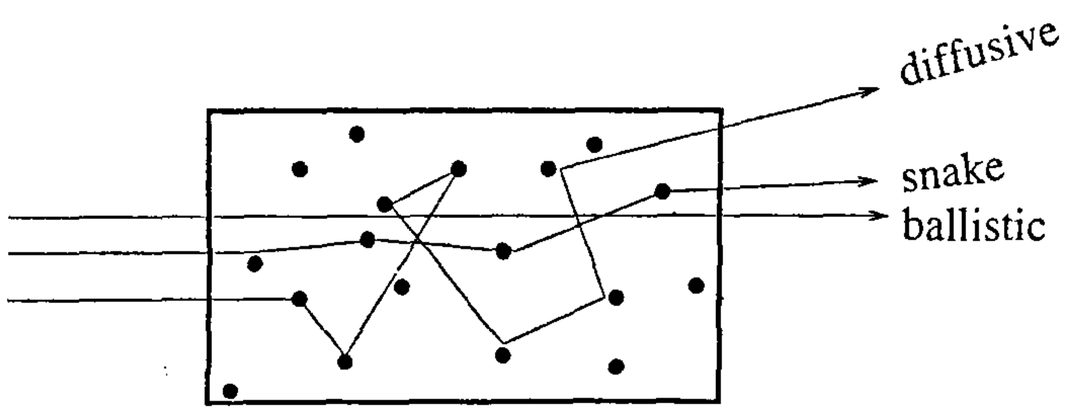

Figure 2. Trajectories of photons in a random medium, showing the ballistic, diffusive and snake components.

hence best for imaging. However, they are few in number, their intensity falling off as $I = I_o \exp(-x/l^*_s)$ where I_o is the input intensity, and x is the distance travelled. The diffuse component, which forms the bulk of the emergent light in turbid media is made up of photons that have undergone random multiple scattering, and these emerge later than the ballistic photons because of their increased path lengths. Their polarization, direction of propagation and phase are completely randomized. For most techniques of imaging, these form the unwanted, incoherent, diffuse background. Snake photons are those that travel in near-forward paths, having undergone few scattering events, all of which are in the forward or near-forward direction. Consequently, they retain the image bearing characteristics to some extent. Due to the varying path lengths the different photons have in the medium, a pulse of light incident on a turbid medium emerges elongated. Typically, a femtosecond pulse is stretched to a picosecond or a nanosecond pulse on travelling through a turbid medium.

All methods of imaging attempt to separate the undeviated ballistic photons from the multiply scattered diffused photons; however, they differ in the method used to achieve this discrimination. While most methods use the ballistic photons to form shadowgrams of objects hidden in turbid media, a few others make use of the diffuse photons to infer about the objects. The rapid advance in this field over the last few years has been possible due to the technological advances, like the availability of femtosecond lasers, fast electronics and very sensitive detectors.

Principles of imaging

The ballistic photons, having travelled a straight, undeviated path in the medium, can form shadows of objects in their path. Thus, if the ballistic photons could be separated from the diffusive, one could obtain shadowgrams of hidden objects. While there are several means of discriminating the ballistic photons in the presence of the diffusive, the most obvious technique appears to be time-gating, which exploits the fact that the diffusive photons arrive later than the ballistic photons. A short, femtosecond pulse is incident on the sample, and the emergent pulse sliced; the first femtosecond slice would form the shadowgram of the object hidden in the turbid medium. As this required fast electronics that were not available in the early 70's, an alternate ingenious method was proposed involving a nonlinear interaction between two beams. One of these is derived from the input femtosecond pulse, while the other is the elongated pulse that has emerged from the turbid medium. Since the nonlinear interaction takes place only in the presence of both pulses, this interaction offers a means for time-gating. A typical set-up employing this technique is shown in Figure 3, where the input pulse is amplitude-divided into two parts. One of these travels through the turbid medium, and falls on the nonlinear medium, while the other follows an alternate route, and reaches the nonlinear medium at the same time as the first one. In the nonlinear medium, the mixing takes place only for the overlap period of the two pulses, which is just the duration of the input pulse. One of the earliest experimental realization of this was by Duguay and Mattick[3], where picosecond time-gating was achieved using Kerr effect. An ultra-fast Kerr shutter was formed by birefringence induced by the ultra-short infrared pulses. The shutter consists of a glass cell containing CS_2 placed between crossed polars (Figure 4). In the absence of any infrared pulse, no light is transmitted. The presence of an infrared pulse induces birefringence, which then permits the input signal light to pass through. Thus, ultra-short infrared pulses can be used to open the shutter for small durations, to permit just the ballistic component of the signal light to pass through. By this technique objects behind scattering media like tissue paper were imaged. Duguay and Mattick also suggested gated ranging in order to estimate the distance of

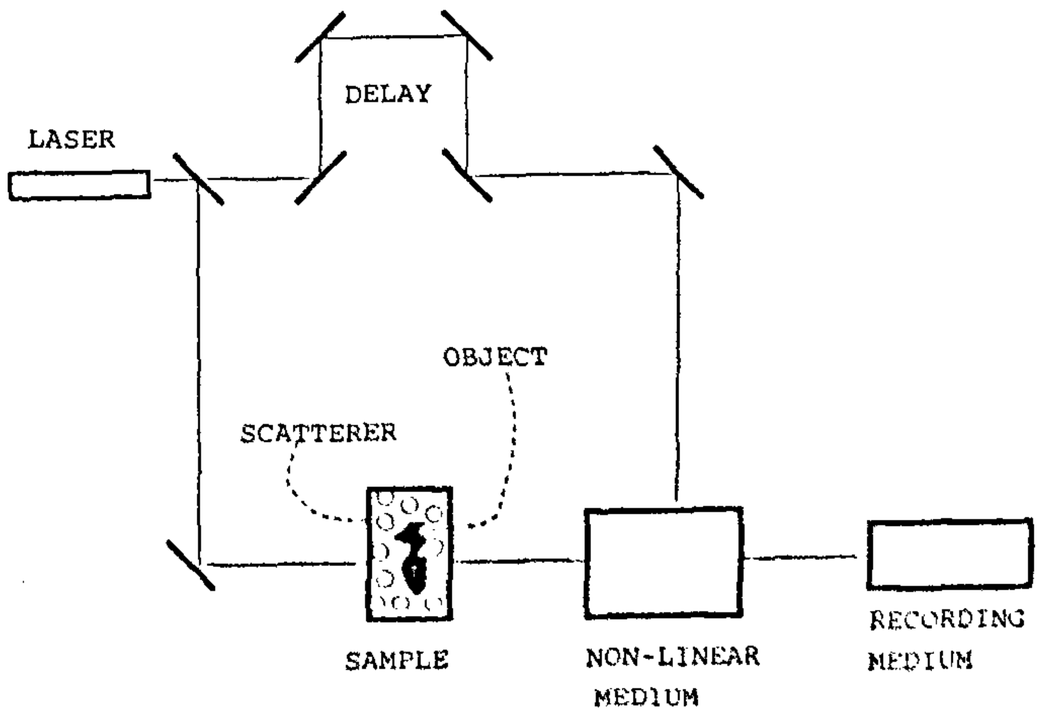

Figure 3. Schematic diagram of an experiment to image through turbid media using a nonlinear process for discrimination.

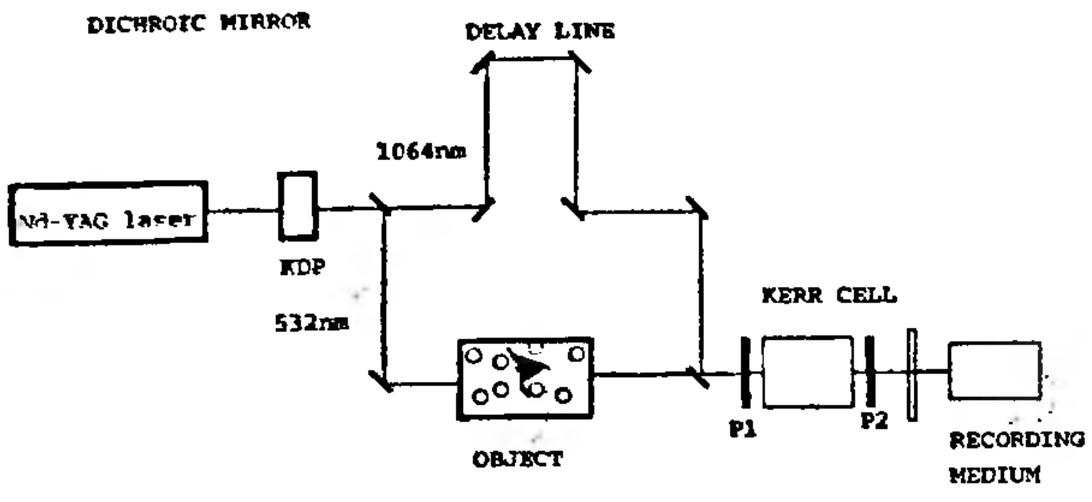

Figure 4. Schematic diagram for imaging using Kerr effect.

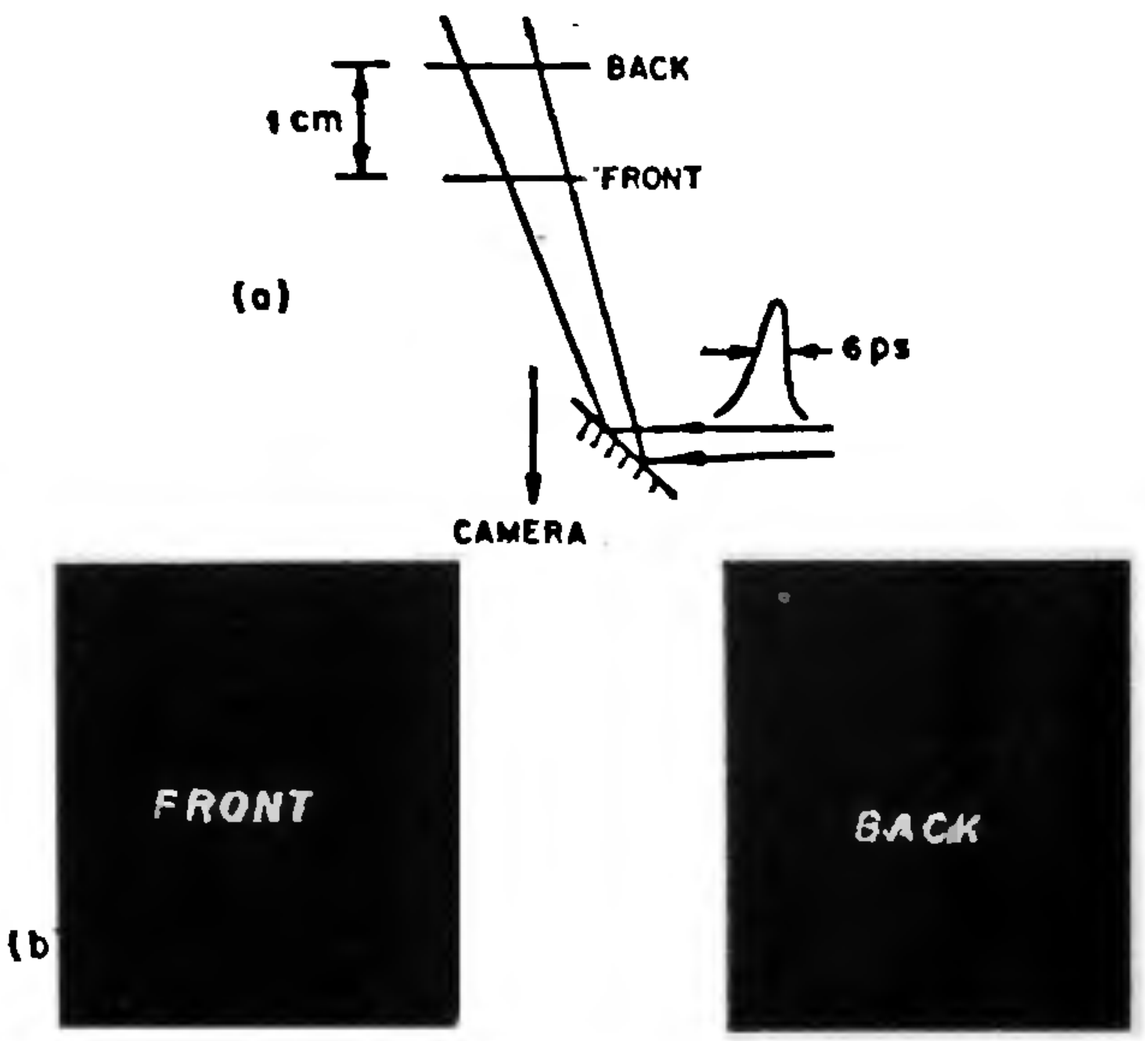

Figure 5. Experimental results of gated imaging of a transparent glass cell with the words 'FRONT' and 'BACK' written on the front and back faces, respectively. The top portion shows the schematic arrangement, where a 6-picosecond pulse is incident on the glass cell. The back-scattered light is directed towards a camera, with a Kerr shutter. The lower portion of the figure shows the gated images of the front and back faces of the cell (from ref. 3).

objects enveloped in scattering media like fog. Short pulses of light may be sent through the fog, and the back-reflected light from the obstacles be recorded by Kerr time-gating. Since just the ballistic part is passed through the Kerr shutter, an image of the scattering object is formed. The opening of the Kerr shutter may be delayed by various times so that the distance to the scattering object may be estimated from the delay time which gives the best image, this being the time taken by the input pulse to travel to the object and back. In a demonstration of gated ranging, they have imaged a glass cell which has the words 'FRONT' and 'BACK' written on the front and back faces respectively. The delay between the light arriving from the front and back faces was calculated, and the shutter opened for picoseconds, after each of the two delays. The resulting images are shown in Figure 5. Thus, nonlinear time-gating appeared to be a very powerful tool for discriminating the ballistic photons from the diffusive. The first medical application of the ultra-fast Kerr shutter is the imaging of an isolated mammalian heart using backscattered light, by Martin and coworkers[4].

Much more progress has been made in Kerr gating. Wang *et al.*[5] have obtained sub-millimeter resolution for two-dimensional imaging of objects placed behind human and chicken tissue, and colloidal suspensions of polystyrene microspheres. They have also reported improvement of signal-to-noise ratio by a factor of 500, and a 3-fold improvement in shutter speed by the use of a double-stage Kerr shutter[6].

In a similar fashion, several other nonlinear processes have been adapted to obtain discrimination of photons. Fujimoto *et al.*[7] employed second harmonic generation to achieve cross-correlation of the reference and the ballistic photons, and have reported femtosecond optical ranging, with 15 μm resolution. This technique was applied in investigating the cornea in a rabbit's eye *in vivo*, and to study the epidermal structure of the human skin *in vitro*. Yoo *et al.*[8] have used second harmonic generation in KDP to achieve 100 femtosecond time-gating.

The nonlinear methods discussed above merely permit transmission or frequency conversion of the ballistic signal, without amplification, often with intensity loss. Duncan *et al.*[9] have demonstrated a technique based on stimulated Raman amplification, where the ballistic photons were amplified by six orders of magnitude in a Raman amplifier, with the long wavelength Stokes beam being amplified by a shorter wavelength pump. The difference in the two wavelengths coincides with a fundamental vibration of the Raman amplifier medium, which in this case was hydrogen gas at 30 atm. The input pulse at the Stokes wavelength was amplitude-divided into the signal and pump pulses. The signal pulse that emerged elongated in time on traversing the turbid medium, was incident on the Raman amplifier, which was strongly pumped by an ultra-short pulse, with an appropriate delay to provide time-gating of the ballistic light. The output of the Raman amplifier had the Stokes signal amplified, resulting in a sensitivity and resolution higher than would have been possible otherwise. A similar technique was employed by Devaux *et al.*[10] where parametric amplification was used for time-gating as well as improvement of the ballistic signal strength.

Meanwhile, by the late 80's fast nanosecond and picosecond detection devices became available, throwing open a vast new area for development of imaging techniques. Delpy *et al.*[11], using a streak camera, studied the propagation of near-infrared light through the head of a

rat. In another study, Das *et al.*[12] employed a high repetition rate 100 fs laser pulse for illumination, and a streak camera for scanning, and imaged a translucent piece of chicken fat embedded in 40 mm thick chicken breast tissue. Another technique of imaging using fast electronics, developed by Andersen-Engels *et al.*[13], adapts delayed coincidence photon counting, where a part of the input pulse was fed to the photon counter, the remaining being incident on the sample. The pulse emerging from the sample was fed to the coincidence counter, and the number of photons arriving after a preset delay time was monitored. In this manner, the ballistic signal could be recorded. In both the streak camera method and the delayed coincidence method, two-dimensional imaging requires a step scan, where at each step the ballistic signal is measured.

The methods discussed so far employ time-gating which selects the ballistic light by virtue of the time of travel in the turbid medium. An alternate approach uses the fact that the input light is coherent, and the ballistic part retains the coherence. Some of the methods which make use of this feature are optical coherence tomography, holography, and coherent anti-Stokes Raman scattering (CARS). Optical coherence tomography is based on the low coherence interferometry, and may be implemented both in retro-reflection and trans-illumination modes. While the former can yield images of microstructures in tissues, the latter may be used to obtain shadows of opaque objects embedded in turbid media. The method uses a broadband light source, and a Michelson interferometer, with the sample in one arm and a mirror in the other (Figure 6). Fringes with good visibility are obtained when the path lengths in the two arms differ to within the coherence length of the source; thus smaller the coherence length of the source, the better the resolution of imaging. By sweeping one arm and simultaneously recording the interference fringes, one can obtain a map of the reflecting surface. In this manner, Izatt *et al.*[14] have imaged *in vitro* the anterior segment of a human eye with micron resolution. Optical coherence tomography has found applications in opthalmology in the study of the corneal and retinal structure[15,16]. This technique has been further developed[17], whereby the dynamic, motion-artifact free *in vivo* image of a beating from a heart was obtained. This was achieved by forming a Michelson interferometer with fibres, and using a piezo-electric fibre-stretcher to vary the reference arm delay.

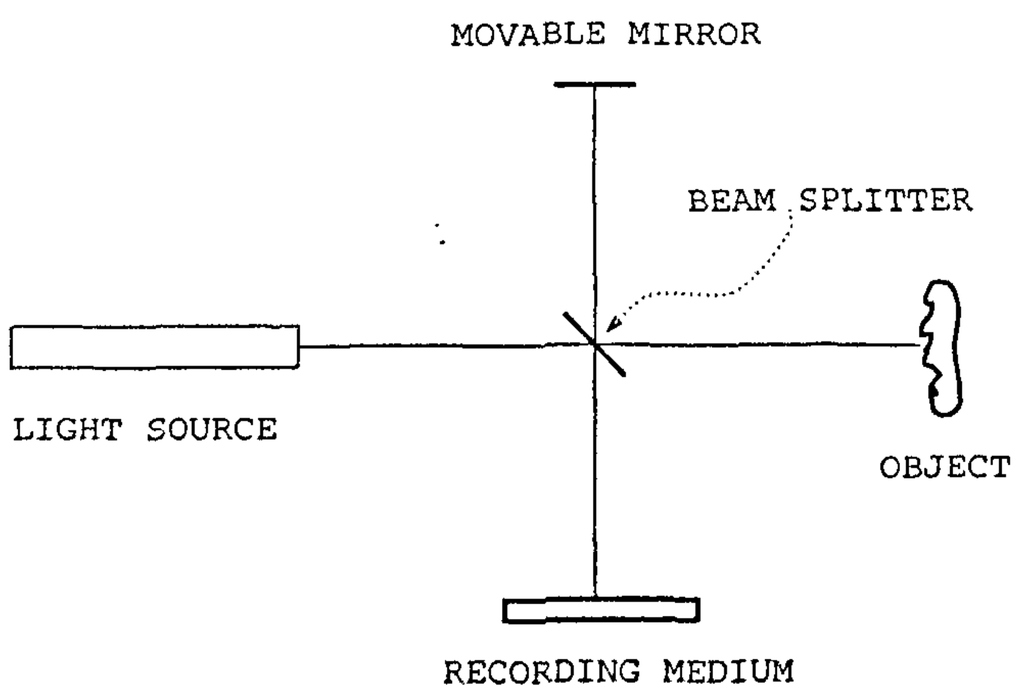

Figure 6. Schematic diagram for optical coherence tomography.

Another method based on optical coherence is the holographic technique, where an ultra-short pulse is split into the object and the reference beams. The object beam traverses the turbid medium and reaches the recording device at the same time as the appropriately delayed reference beam. The interference pattern is recorded, with a meaningful pattern being formed during the overlap period of the two beams. Thus, the ballistic component contributes to the holographic recording, while the later arriving diffuse light forms incoherent noise, exposing the recording medium and reducing the fringe visibility. Considerable work in this field has been carried out by Abramsons and Spears[18] and Leith *et al.*[19,20]. In the initial investigations, photographic media were used, which have now been replaced by CCD cameras, giving rise to the term 'electronic holography'.

As work in this field grew in volume, several other results were established. It was recognized that spatial filtering, to some extent, was equivalent to time-gating[19–21]. A spatial filter is formed by a lens–aperture system, with a lens of focal length f which collects light and focuses it onto an aperture of radius a placed at its focus (Figure 7). Since light travelling along the axis is focussed onto the aperture and transmitted, while light travelling in other directions is focussed off the aperture, and is blocked, the spatial filter may be used to cut off, to some extent, the diffuse light that travels in all directions, while transmitting the on-axis ballistic light. Similarly, attention was also focused on the polarization characteristics of the diffusive light, and it was conclusively established that discrimination could be carried out based on polarization. Several schemes have been devised that utilize the fact that the ballistic light preserves the initial direction of propagation and polarization. Implementation of spatial filtering and polarization discrimination was found to aid in the sensitivity and resolution[22–24].

Almost all work has concentrated on the use of a pulsed source of light, and in contrast, there has been very little work using continuous wave sources. This is because the diffusive part of an earlier portion of the input light would overlap with the ballistic photons from a later part of the input light, making the separation

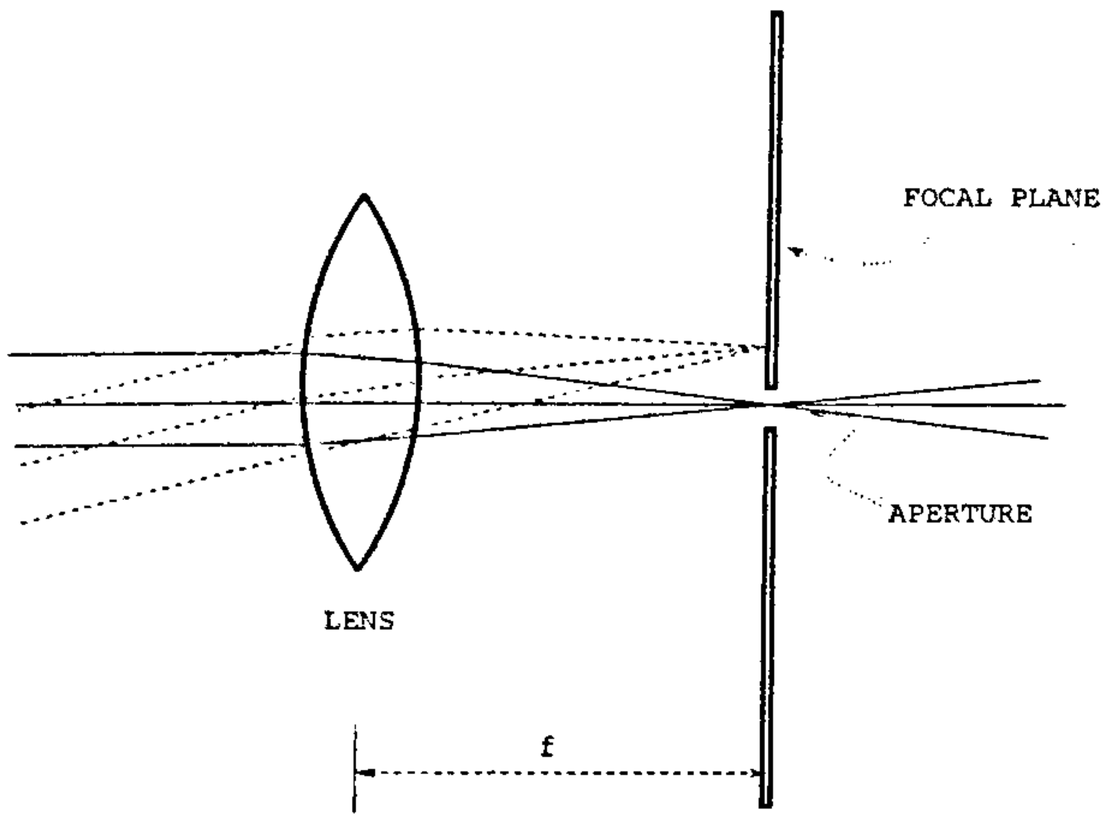

Figure 7. A spatial filter formed by a lens and an aperture at its focal point.

impossible by the methods discussed so far. Early work on continuous wave sources used intensity-modulated continuous wave light[25], which gives rise to a diffuse photon density wave that has a well-defined wavelength, amplitude and phase at all points in the medium. The scattering of these waves by hidden objects is measured by detectors placed all around the sample, and imaging is considered an inverse source problem.

Horinaka *et al.*[23] have shown that ballistic and snake photons can be extracted by continuous wave sources using light polarization. They established the equivalence of temporal gating using pulsed sources and polarization discrimination using continuous wave polarization-modulated sources. While Demos and Alfano[24,26] have used polarization discrimination to obtain images using pulsed sources, Emile *et al.*[27] have obtained images using continuous wave light from a 30 mW dye laser. Their scheme (Figure 8) uses a linearly polarized source, with the plane of polarization rotating at some angular frequency. Two pinholes, one in front of the sample, and one behind, define the direction of propagation. Light emerging from the exit pinhole passed through a fixed analyser, and was detected by a photomultiplier tube, the output of which was passed to a lock-in amplifier that locked onto the frequency corresponding to that of the input polarization rotation frequency, thus picking out the ballistic component (and to some extent the snake) in the presence of the diffusive. By a synchronized step-scan of the two pinholes, they have obtained images of a millimeter-sized object immersed in milk. This was a significant achievement, as it used easily available continuous wave sources, and did not require very sophisticated electronic devices.

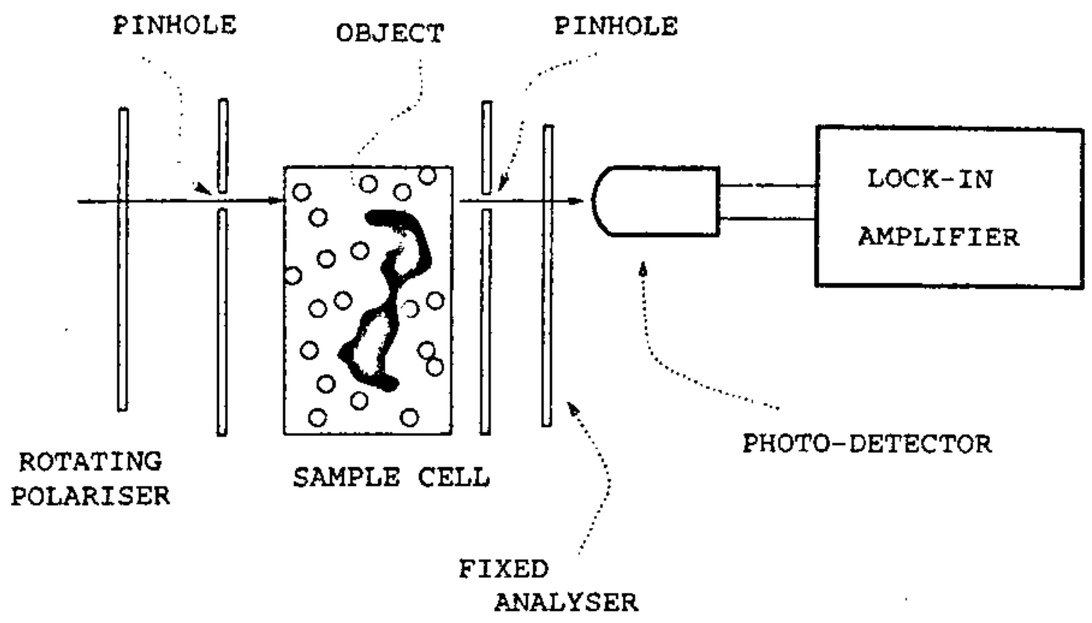

Figure 8. Imaging scheme using a continuous wave light source, with polarization discrimination and step scan.

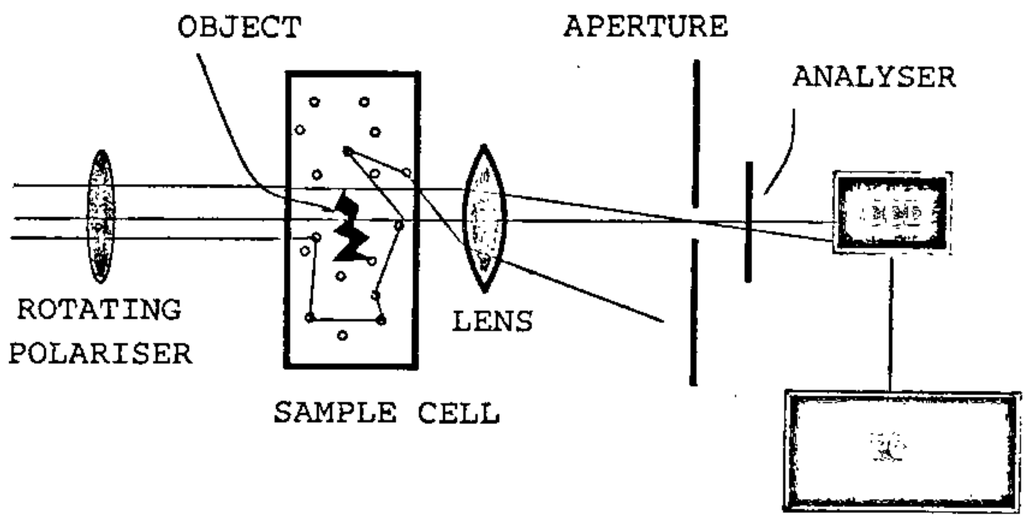

Figure 9. An imaging scheme for two-dimensional imaging through turbid media using a continuous wave source.

Recently, we have devised a method[28] of rapid two-dimensional imaging using low power continuous wave sources. The technique uses a combination of spatial filtering and polarization discrimination, separating out the ballistic photons by virtue of the fact that these have retained their polarization, and direction of propagation, while the diffusive photons have not. Light from a continuous wave source like a low-power HeNe laser or a diode laser is polarization-modulated by a rotating linear polarizer, or half wave plate, and is incident on the sample (Figure 9). The light emerging from the sample is spatially filtered and passed through a fixed analyser onto a CCD camera that rapidly acquires a sequence of frames. These frames are two-dimensional intensity data, with the successive frames differing in that the direction of input polarization was different. The polarization discrimination is achieved by Fourier transforming the time sequence of images to extract the component that has the same frequency of variation as the input polarization modulation. This is the ballistic component (and to some extent the snake). By this

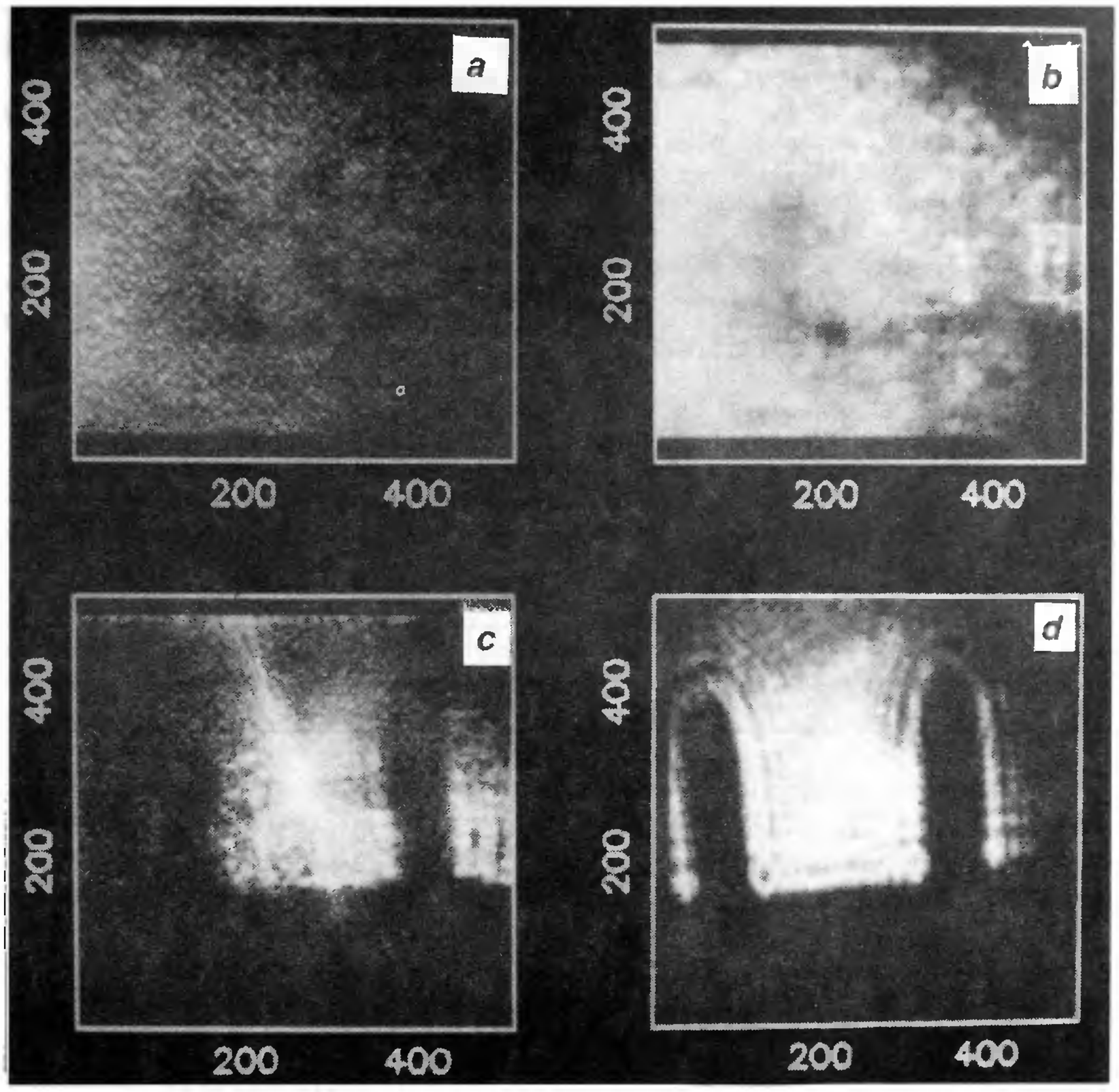

Figure 10. Experimental realization of imaging using a HeNe laser[28]. *a*, A typical frame recorded by the CCD camera. No object is visible; *b*, The zero-frequency component after Fourier transform. The hexagonal structures are the cells on the face plate of the CCD camera. The dark spot is a defective region on the face plate of the CCD; *c*, The image of the object (a portion of an IC) obtained at the frequency 2ω. Note that even some diffraction lines are seen; and *d*, The bare object, with no scattering medium.

technique, using a 1 mW HeNe laser, we have obtained better than 100 μm resolution imaging of millimeter-sized objects immersed in turbid media that are more than 30 transport mean free paths thick (Figure 10). Direct formation of two-dimensional images, the absence of synchronized stepping parts and polarization discrimination by software in post-processing contribute to the speed and ease of data collection. The use of diode lasers makes the equipment compact and portable, an advantage in medical and field applications.

Conclusions

Imaging through turbid media has become a field of intense activity, and rapid progress has been made using different techniques which have demonstrated numerous applications. Although the basic physics in this field was known for a long time, practical implementation had to wait for technology to provide suitable devices like femtosecond lasers, fast detection devices, and two-dimensional array cameras. Intense efforts are currrently being directed towards improving detection capability and resolution.

1. Ertefai, S. and Profio, A. E., *Med. Phys.*, 1985, **12**, 393.
2. Peters, V. G. *et al.*, *Phys. Med. Biol.*, 1990, **35**, 1317.
3. Duguay, M. A. and Mattick, A. T., *Appl. Opt.*, 1971, **10**, 2162–2170.
4. Martin, J. L., Lecarpentier, Y., Antonetti, A. and Grillon, G., *Med. Biol. Eng. Comput.*, 1980, **18**, 250.
5. Wang, L., Ho, P. P., Liu, C., Zhang, G. and Alfano, R. R., *Science*, 1991, **253**, 769–771.
6. Wang, L. M., Ho, P. P. and Alfano, R. R., *Appl. Opt.*, 1993, **32**, 535–539.
7. Fujimoto, J. G., de Silvestri, S., Ippen, E. P., Puliafito, C. A., Margolis, R. and Oseroff, A., *Opt. Lett.*, 1986, **11**, 150–152.

8. Yoo, K. M., Xing, Q. and Alfano, R. R., *Opt. Lett.*, 1991, **16**, 1019.
9. Duncan, M. D., Mahon, R., Tankersley, L. L. and Reintjes, J., *Opt. Lett.*, 1991, **16**, 1868–1870.
10. Devaux, F., Lantz, E. and Malliotte, H., *Opt. Commun.*, 1995, **114**, 295.
11. Delpy, D., Cope, M., van der Zee, P., Arridge, S., Wray, S. and Wyatt, J., *Phys. Med. Biol.*, 1988, **33**, 1433.
12. Das, B. B., Yoo, K. M., Alfano, R. R., *Opt. Lett.*, 1993, **18**, 1092–1094.
13. Andersen-Engels, S., Berg, R., Svanberg, S. and Jarlman, O., *Opt. Lett.*, 1990, **15**, 1179–1181.
14. Izatt, J. A., Hee, M. R., Huang, D., Swanson, E. A., Lin, C. P., Schuman, J. S., Puliafito, C. A. and Fujimoto, J. G., *Optics and Photonics News*, October 1993, p. 14.
15. Hee, M. R., Izatt, J. A., Swanson, E. A., Huang, D. Lin, C. P., Schuman, J. S., Puliafito, C. A. and Fujimoto, J. G., *Arch. Opthalmol.*, 1995, **113**, 325.
16. Puliafito, C. A., Hee, M. R., Lin, C. P., Reichel, E., Schuman, J. S., Duker, J. S., Izatt, J. A., Swanson, E. A. and Fujimoto, J. G., *Opthalmology*, 1993, **102**, 217.
17. Tearney, G. J., Bouma, B. E., Boppart, S. A., Golubovic, B., Swanson, E. A. and Fujimoto, J. G., *Opt. Lett.*, 1996, **21**, 1408–1140.
18. Abramson, N. H. and Spears, K. G., *Appl. Opt.*, 1989, **28**, 1834.
19. Leith, E., Arons, E., Chen, H., Chen, Y., Dilworth, D., Lopez, J., Shih, M., Sun, P. C. and Vossler, G., *Optics and Photonics News*, Oct. 1993, 19–23.
20. Chen, H., Chen, Y., Dilworth, D., Leith, E., Lopez, J. and Valdmanis, J., *Opt. Lett.*, 1991, **16**, 487–489.
21. Wang, Q. Z., Liang, X., Wang, L., Ho, P. P. and Alfano, R. R., *Opt. Lett.*, 1995, **20**, 1498–1500.
22. Wang, L., Ho, P. P. and Alfano, R. R., *Appl. Opt.* 1989, **28**, 2304.
23. Horinaka, H., Hashimoto, K., Wada, K. and Cho, Y., *Opt. Lett.*, 1995, **20**, 1501–1503.
24. Demos, S. G. and Alfano, R. R., *Opt. Lett.*, 1996, **21**, 161–163.
25. O'Leary, M. A., Boas, D. A., Chance, B. and Yodh, A. G., *Phys. Rev. Lett.*, 1992, **69**, 2658.
26. Demos, S. G. and Alfano, R. R., *Appl. Opt.*, 1997, **36**, 150–155.
27. Emile, O., Bretenaker F. and le Floch, A., *Opt. Lett.*, 1996, **21**, 1706–1708.
28. Hema Ramachandran and Andal Narayanan, *Opt. Commun.*, 1998, **154**, 255–260.

ACKNOWLEDGEMENTS. I am indebted to Prof. N. Kumar, who introduced me to this subject, and to Prof. Rajaram Nityananda, with whom I had many useful discussions. I also wish to thank Dr Andal Narayanan with whom I worked on the imaging experiment.